ERJ Express. Published on January 22, 2009 as doi: 10.1183/09031936.00101408

Role of Lymphotoxin-α in Cigarette Smoke-Induced Inflammation and Lymphoid Neogenesis

Tine Demoor[1], Ken R. Bracke[1], Tania Maes[1], Bernard Vandooren[2], Dirk Elewaut[2], Charles Pilette[3], Guy F. Joos[1] and Guy G. Brusselle[1]

[1]Department of Respiratory Medicine, Laboratory for Translational Research in Obstructive Pulmonary Diseases, Ghent University Hospital, Ghent, Belgium.

[2]Department of Rheumatology, Laboratory of Molecular Immunology and Inflammation, Ghent University Hospital, Ghent, Belgium.

[3]Unit of Pneumology and Microbiology, Department of Pneumology, Cliniques Universitaires St-Luc, Université Catholique de Louvain (UCL), Brussels, Belgium.

Address correspondence and reprint requests to Dr. Guy G. Brusselle, Department of Respiratory Medicine, Ghent University Hospital 7K12E, De Pintelaan 185, 9000 Ghent, Belgium. Fax: +32 (0)9 332 23 41. E-mail-address: guy.brusselle@ugent.be

This work was supported by the Concerted Research Action of the University of Ghent (BOF/GOA 01251504). Dr. Bernard Vandooren is a research assistant of the Fund for Scientific Research Flanders (FWO-Vlaanderen). Dr. Ken Bracke is a postdoctoral fellow of the Fund for Scientific Research Flanders. Dr. Tania Maes is a postdoctoral fellow sponsored by the Interuniversity Attraction Poles Program/Belgian State/Belgian Science Policy (P6/35).

Running title: Cigarette smoke-induced lymphoid neogenesis

Word count abstract: 200

Word count text: 3623

Number of figures: 8

Abstract

In chronic obstructive pulmonary disease (COPD), chronic inflammation is accompanied by peribronchial lymphoid aggregates. Lymphotoxin-α (LTα), crucial in secondary lymphoid organogenesis, may be involved in lymphoid neogenesis.

We examined cigarette smoke (CS)-induced pulmonary lymphoid neogenesis and inflammation *in vivo* in LTα knockout ($LT\alpha^{-/-}$) and wild-type (WT) mice and studied expression of lymphoid chemokines by lung fibroblasts *in vitro*.

T-cell numbers (in bronchoalveolar lavage fluid (BALF) and lungs) and lymphoid aggregate numbers were significantly higher in air-exposed $LT\alpha^{-/-}$ mice than in WT animals, and increased upon chronic CS exposure in both genotypes. In contrast, local IgA responses upon chronic CS exposure were attenuated in $LT\alpha^{-/-}$ mice. CXCL13 and CCL19 mRNA in total lung and CXCL13 protein level in BALF increased upon CS exposure in WT, but not in $LT\alpha^{-/-}$ mice. *In vitro* lymphotoxin-β receptor (LTβR) stimulation induced CXCL13 and CCL19 mRNA in WT lung fibroblasts. Furthermore, *in vitro* exposure to cigarette smoke extract (CSE) up-regulated CXCL13 mRNA expression in WT, but not in $LT\beta R^{-/-}$, lung fibroblasts.

In this murine model of COPD, CS induces pulmonary expression of lymphoid chemokines CXCL13 and CCL19 in a LTαβ-LTβR-dependent fashion. However, LTα is not required for CS-induced pulmonary lymphocyte accumulation and neogenesis of lymphoid aggregates.

Key words: chronic obstructive pulmonary disease, cigarette smoking, cytokines and chemokines, lymphotoxin alpha, mouse models

Introduction

Chronic obstructive pulmonary disease (COPD) is characterized by a slowly progressive airflow limitation that is poorly reversible (1). COPD is one of the leading causes of death with cigarette smoking as main risk factor (2). The molecular and cellular mechanisms responsible for the development of COPD are poorly understood. For that reason, a murine smoke-model of COPD was developed, showing a pulmonary pathology comparable to the disease in COPD patients (3), including inflammation and remodeling of the small airways as well as destruction of the lung parenchyma, emphysema.

Recently we (4),as well as others (5), reported the appearance of lymphoid aggregates in murine lung tissue upon chronic cigarette smoke (CS) exposure. Similar lymphoid follicles with clearly delineated T- and B-cell areas can be seen in lung sections of patients with severe COPD (6;7). The underlying mechanisms and functional properties of lymphoid follicle formation in the lung remain to be elucidated.

Lymphotoxin-α (LTα), essential in organogenesis of secondary lymphoid organs, may induce the development of tertiary lymphoid tissue. LTα knockout ($LT\alpha^{-/-}$) mice have no lymph nodes or Peyer's patches and aberrant splenic architecture (8;9), while site-specific LTα expression in transgenic animals causes local inflammation with a cellular composition and organization similar to those of lymph nodes (10).

LTα exists as a soluble homotrimer ($LT\alpha_3$) or as a membrane-bound heterotrimer with lymphotoxin β ($LT\alpha_1\beta_2$). $LT\alpha_3$, produced by activated T-cells and early B-cells, is functionally redundant with TNF-α (11). $LT\alpha_1\beta_2$ on activated T- and B-lymphocytes and natural killer (NK) cells, binds exclusively to the TNFR-like LTβ receptor (LTβR), on stromal and myeloid lineage cells (12). The LTαβ-LTβR pathway is crucial in lymphoid organ development and triggers the expression of lymphoid chemokines, such as CXCL12,

CXCL13, CCL19 and CCL21 (13;14). Furthermore, this LTαβ-LTβR pathway has been implicated in the thymic emigration of (Vα14) Invariant Natural Killer T (iNKT) cells (15).

To reveal the *in vivo* role of LTα in CS-induced inflammation, pulmonary emphysema, lymphoid neogenesis and mucosal IgA production, we subjected wild-type (WT) and LTα$^{-/-}$ mice to subacute (4 weeks) or chronic (24 weeks) CS exposure. Moreover, we studied *in vitro* the expression of lymphoid chemokines by lung fibroblasts under baseline conditions and upon stimulation with agonistic LTβR Ab and/or cigarette smoke extract (CSE).

Materials and Methods

Animals

Homozygous male C57Bl/6 LTα$^{-/-}$ (LTa^{tm1Dch}) mice and C57Bl/6 WT mice (8 weeks old) were obtained from The Jackson Laboratory (Bar Harbor, ME, USA) (8). The local Ethics Committee for animal experimentation of the faculty of Medicine and Health Sciences (Ghent, Belgium) approved all *in vivo* manipulations.

Smoke exposure

Mice (n = 8 per group) were exposed to cigarette smoke (CS), as described previously (16). Briefly, groups of 8 mice were exposed whole body to the tobacco smoke of 5 cigarettes (Reference Cigarette 2R4F without filter, University of Kentucky, Lexington, KY, USA), four times a day with 30 minutes smoke-free intervals, 5 days a week for 4 weeks (subacute exposure) or 24 weeks (chronic exposure). During the exposure an optimal smoke:air ratio of 1:6 was obtained. The control groups were exposed to air. Carboxyhemoglobin in serum of smoke-exposed mice reached a non-toxic level of 8.3 ± 1.4% (compared with 1.0 ± 0.2% in air-exposed mice, n = 7 for both groups), similar to carboxyhemoglobin blood concentrations of human smokers (17).

Bronchoalveolar lavage (BAL)

24 hours after the last exposure, mice were euthanized with an overdose of pentobarbital and BAL fluid was collected, as described previously (16). A total cell count was performed in a Bürker chamber, and differential cell counts (on at least 400 cells) were performed on cytocentrifuge preparations using standard morphologic criteria after May-Grünwald-Giemsa

staining. Flow cytometric analysis of BAL cells was performed to enumerate dendritic cells (DCs) and $CD4^+$ and $CD8^+$ T lymphocytes.

Preparation of lung single-cell suspensions

After rinsing of pulmonary and systemic circulation, the left lung was used for histology, and the right lung for the preparation of a single cell suspension, as detailed previously (16). Cell counting was performed with a Z2 Beckman Coulter particle counter (Beckman Coulter, Ghent, Belgium).

Labelling of BAL cells and single cell-suspensions for flow cytometry

The following mAbs were used to identify mouse dendritic cell (DC) populations: anti-CD11c-APC (HL3) and anti-I-A^b-PE (AF6-120.1). We discriminated between macrophages and myeloid DCs using the methodology described by Vermaelen and Pauwels (18). The following mAbs were used to stain mouse T cell subpopulations: anti-CD4-FITC (GK1.5), anti-CD8-FITC (53-6.7), anti-CD3-APC (145-2C11) and anti-CD69-PE (H1.2F3). Using anti-CD19-PE (1D3) and anti-CD11c, B lymphocytes were identified as the CD11c-low and CD19-positive population. All mAbs were obtained from BD Pharmingen. iNKT cells were stained with anti-CD3 and PE-conjugated CD1d tetramer loaded with α-galactosylceramide (αGalCer) (19). In a last step before analysis, cells were incubated with 7-aminoactinomycin D (or viaprobe; BD Pharmingen) to check cell viability. Flow cytometry data acquisition was performed on a FACScalibur™ running CellQuest™ software (BD Biosciences). FlowJo software was used for data analysis (TreeStar Inc., Ashland, OR, USA).

Histology

The left lung was fixated by intratracheal infusion of fixative (4% paraformaldehyde), as described previously (16). The lung lobe was embedded in paraffin and cut into 3-μm transversal sections. Photomicrographs were captured using a Zeiss KS400 image analyzer platform (KS400, Zeiss, Oberkochen, Germany).

Quantification of pulmonary emphysema

To evaluate pulmonary emphysema, we determined the enlargement of the alveolar spaces by measuring the mean linear intercept (L_m), as described previously (4;16). Using image analysis software (ImageJ 1.34s) a 100 x 100-μm grid was placed over images of hematoxylin&eosin-stained lung sections, acquired and scored in a blinded fashion. The total length of each line of the grid divided by the number of alveolar intercepts gives the average distance between alveolated surfaces, the L_m.

Morphometric quantification of lymphoid infiltrates

To evaluate the presence of lymphoid infiltrates in lung tissues, sections obtained from formalin-fixed, paraffin-embedded lung lobes were subjected to an immunohistological CD3/B220 double-staining as described previously (4). Infiltrates in the proximity of airways and blood vessels were counted. Dense accumulations of at least 50 cells were defined as lymphoid aggregates. Counts were normalized for the number of bronchovascular bundles per lung section.

Immunohistochemistry for CXCL13

Paraffin sections were incubated with primary anti-CXCL13 Ab (R&D Systems, Minneapolis, MN, USA), followed by biotinylated rabbit anti-goat-Ab from the Vectastain Elite ABC kit

(Vector Laboratories, Burlingame, CA, USA). After incubation with streptavidin-horseradish peroxidase, slides were coloured with diaminobenzidine (Dako, Carpinteria, CA, USA) and counterstained with Mayer's hematoxylin (Sigma-Aldrich, St. Louis, MO, USA).

ELISA

Commercially available ELISA kits were used to determine CXCL13 and CCL21 protein levels in BALF (R&D Systems) as well as IgM (ZeptoMetrix, Buffalo, NY, USA) and IgA (Alpha Diagnostic International, San Antonio, TX, USA) titers in serum and BALF. Secretory-IgA (S-IgA) was measured with a sandwich ELISA, developed in the laboratory of co-author CP. BALF samples were assayed using a polyclonal goat antibody to rat secretory component (SC), cross-reactive with mouse SC, as capture antibody and biotinylated anti-mouse IgA (Sigma-Aldrich) as detection antibody. S-IgA data were expressed as corrected OD, in the absence of a murine standard.

RT-PCR analysis

Total lung RNA was extracted with the RNeasy Mini Kit (Qiagen, Hilden, Germany). RNA from cultured cells was extracted with the ChargeSwitch Total RNA Cell Kit (Invitrogen Corp, Carlsbad, CA, USA). Expression of CXCL13, CCL19, CCL20, CXCR5 and CCR7 mRNA, relative to hypoxanthine guanine phosphoribosyltranferase (hprt) mRNA, was analyzed with the Assays-on-Demand Gene Expression Products (Applied Biosystems, Foster City, CA, USA). RT-PCR was performed on a LightCycler 480 Instrument (Roche Diagnostics, Basel, Switzerland) with murine leukemia virus RTase (Applied Biosystems) under previously described conditions (4).

Lung fibroblast culture

Lungs from a WT and a LTβR$^{-/-}$ mouse (20) (C57Bl/6) were digested, as described above, into single-cell suspensions. Cells were seeded in DMEM supplemented with 10% FBS, *L*-glutamine and penicillin/streptomycin (all from Gibco BRL, Invitrogen Corp) and incubated in a humidified 37°C incubator with 5% CO_2. 24 hrs after plating, non-adherent cells were removed by medium change. Cells were passaged at subconfluency. At passage 5, fibroblastic phenotype was checked on Lab-Tek chamber slides (Nalge Nunc, Rochester, NY, USA). In addition to positive staining of the cells for vimentin with monoclonal anti-vimentin Ab (clone VIM 13.2, Sigma-Aldrich), fibroblast morphology was confirmed by inverted phase-contrast microscopy.

Stimulation of cultured lung fibroblasts

At passage 6, cells were plated onto 24-well plates at a density of $4x10^4$ cells/well and grown to confluency. Cells were stimulated for 48 hrs with 1 ml culture medium, isotype control (2 μg/ml), agonistic LTβR Ab (2 μg/ml), 5% cigarette smoke extract (CSE), or the combination of agonistic LTβR Ab with CSE. 100% CSE was prepared as described previously (21). Agonistic LTβR Ab consisted of a 9:1 mix of 4H8 and 3C8 (Carl F. Ware, La Jolla Institute, San Diego, CA, USA). Isotype control consisted of a 9:1 mix of rat IgG_{2a} (A110-2) and rat IgG_1 (R3-34) (BD Pharmingen).

Statistical analysis

Reported values are expressed as mean ± SEM. Statistical analysis was performed with Sigma Stat software (SPSS 15.0 Inc, Chicago, IL, USA) using nonparametric tests (Kruskall-Wallis; Mann-Whitney *U*). A p value ≤ 0.05 was considered significant.

Results

Modulation of CS-induced inflammation in BAL fluid of LTα$^{-/-}$ mice

Subacute and chronic CS exposure increased the number of total cells, alveolar macrophages, dendritic cells (DCs), neutrophils and lymphocytes in the BAL fluid of both WT and LTα$^{-/-}$ mice, compared to air-exposed animals (Fig. 1). Neutrophilic inflammation was significantly attenuated in LTα$^{-/-}$ mice at both time points (Fig. 1 *D*). In contrast, baseline levels of BAL lymphocytes, more specifically both CD4^{+} and CD8^{+} T-cells, were significantly higher in air-exposed LTα$^{-/-}$ mice than in WT mice, and increased further upon CS exposure (Fig. 1, *E* and *F*).

CS-induced pulmonary inflammation and emphysema

The CS-induced increase in lung macrophages and DCs was comparable between WT and LTα$^{-/-}$ mice (Fig. 2, *A* and *B*). Baseline B- and T-cell numbers were higher in the lungs of air-exposed LTα$^{-/-}$ mice versus WT mice. Contrary to the B-cell numbers, T-cell numbers increased strongly upon chronic CS exposure in the lung compartment of both WT and LTα$^{-/-}$ mice (Fig. 2, *C* and *D*).

In both WT and LTα$^{-/-}$ mice, chronic CS exposure induced significantly higher numbers of activated CD4^{+}CD69^{+} and CD8^{+}CD69^{+} T-cells. Yet again, both cell types were significantly increased in air-exposed LTα$^{-/-}$ mice in comparison with WT mice (Fig. 2, *E* and *F*). These steady state differences in lymphocyte numbers, between air-exposed WT and LTα$^{-/-}$ mice, were confirmed in the short term experiment (data not shown).

The L_m increased significantly upon chronic CS exposure in WT mice (air, 34.55 ± 0.35 μm vs. smoke, 37.35 ± 0.71 μm; 8,1% increase; p = 0,037) as in LTα$^{-/-}$ mice (air, 33.71 ± 0.50 μm

vs. smoke, 36.71 ± 0.82 μm; 8,9% increase; p = 0,009). There was no significant difference in L_m between CS-exposed WT and LTα$^{-/-}$ mice (p = 0,505).

Increase of iNKT cells in the lung upon subacute CS exposure is LTα-dependent

iNKT cell numbers were determined through high specificity binding to CD1d-tetramer loaded with αGalCer (19) (Fig. 3 *A*). Subacute CS exposure caused a significant increase of iNKT cells in WT but not in LTα$^{-/-}$ mice (Fig. 3, *B* and *C*). In contrast, chronic CS exposure did not change iNKT cell numbers in the WT and knockout mice, but LTα$^{-/-}$ mice had lower percentages of iNKT cells compared to WT mice (Fig. 3, *D* and *E*).

LTα is not required for lymphoid neogenesis upon chronic CS exposure

Lymphoid aggregates were scarce in lung sections of air-exposed WT mice (Fig. 4, *A* and *B*), whereas the lungs of air-exposed LTα$^{-/-}$ mice were strongly infiltrated with lymphocytes. (Fig. 4, *A* and *D*). Chronic (24 weeks) CS exposure significantly increased the number of peribronchial and perivascular lymphoid aggregates in the lungs of both WT and LTα$^{-/-}$ mice (Fig. 4, *A-E*). Lymphoid aggregates were absent in the lungs of WT mice after subacute (4 weeks) exposure to air or CS (data not shown). In contrast, lungs of air-exposed LTα$^{-/-}$ mice already showed a high degree of lymphocyte infiltration, but short term CS exposure did not induce additional aggregates (# aggregates / # bronchovascular bundles: air-exposed LTα$^{-/-}$ mice: 0,31 ± 0,059, CS-exposed LTα$^{-/-}$ mice: 0,28 ± 0,054; means ± SEM, n = 5 animals/group).

Local and systemic IgA response upon chronic CS exposure is attenuated in LTα$^{-/-}$ mice

Serum and BALF IgA levels were significantly diminished in LTα$^{-/-}$ mice compared to WT animals, both at baseline in air-exposed mice and upon CS exposure for 24 weeks (Fig. 5). In serum, the relative increase in IgA levels upon chronic CS exposure was larger in the LTα$^{-/-}$ mice compared to WT (Fig. 5*A*), whereas in BALF, the opposite was observed (Fig. 5*B*). Chronic CS exposure increased secretory IgA (S-IgA) levels in BALF of WT mice, while BALF S-IgA levels in LTα$^{-/-}$ mice were significantly lower, both in air- and CS-exposed animals (Fig. 5*C*), indicating impairment of S-IgA responses. In contrast, IgM levels were higher in serum and BALF of LTα$^{-/-}$ mice, both at baseline and upon CS exposure (Fig. 5, *D* and *E*).

LTα affects chemokine expression upon CS exposure

mRNA expression of CXCL13 and CCL19 was significantly increased in total lung after CS exposure in WT animals, whereas this increase could not be seen in LTα$^{-/-}$ mice (Fig. 6, *A* and *B*). mRNA levels of CCL20/MIP-3α, an attractant for immature DCs and lymphocytes, were increased in lungs of WT mice upon CS exposure (Fig. 6*C*). Baseline MIP-3α expression was higher in LTα$^{-/-}$ mice compared to WT mice, with a strong tendency to increase after chronic CS exposure (p = 0,076).

Total lung mRNA levels of CXCR5 and CCR7, the receptors for CXCL13 and CCL19 respectively, were higher at baseline in LTα$^{-/-}$ mice (CXCR5: WT = air, 0.28 ± 0.045 vs. smoke, 0.36 ± 0.065; LTα$^{-/-}$ mice = air, 2.09 ± 0.52 vs. smoke, 1.74 ± 0.26; CCR7: WT = air, 0.39 ± 0.038 vs. smoke, 0.73 ± 0.086; LTα$^{-/-}$ mice = air, 1.29 ± 0.19 vs. smoke, 1.33 ± 0.16). CCR7 mRNA expression increased upon subacute CS exposure in WT, but not in LTα$^{-/-}$ mice.

CXCL13 protein levels in BALF were up-regulated upon subacute and chronic CS exposure, again only in WT mice (Fig. 6*D*). Immunohistochemistry in WT mice revealed CXCL13 expression in CS-induced lymphoid aggregates (Fig. 6*E*). CS exposure did not affect protein levels of total CCL21 in BAL fluid of both WT and LTα$^{-/-}$ mice (data not shown).

In vitro expression of CXCL13 and CCL19 in lung fibroblasts is LTβR-mediated

To reveal the mechanism by which CXCL13 and CCL19 are induced in the lung, we stimulated cultured WT and LTβR$^{-/-}$ lung fibroblasts with agonistic LTβR Ab and/or CSE.

In WT lung fibroblasts, *in vitro* stimulation with agonistic LTβR Ab or CSE resulted respectively in a 60-fold and 5-fold increase in expression of CXCL13 mRNA. Furthermore, the combination of LTβR Ab with CSE induced a 100-fold up-regulation in CXCL13 mRNA levels (Fig. 7*A*). A similar CCL19 mRNA response was seen upon stimulation with LTβR Ab or LTβR Ab with CSE combined, but there was no significant effect of CSE exposure alone (Fig. 7*C*). The different stimulations did not affect CXCL13 and CCL19 mRNA expression in LTβR$^{-/-}$ lung fibroblasts (Fig.7, *B* and *D*), however, baseline mRNA levels of both CXCL13 and CCL19 were higher compared to WT lung fibroblasts (data not shown).

Discussion

Using *in vivo* studies with WT and LTα$^{-/-}$ mice, we have demonstrated for the first time that CS-induced pulmonary lymphocyte accumulation and lymphoid neogenesis do not require LTα. Moreover, LTα$^{-/-}$ mice are not protected against the development of CS-induced emphysema. In contrast, LTα is required for CS-induced up-regulation, but not for baseline expression, of the lymphoid chemokines CXCL13 and CCL19. We have shown *in vitro* that the up-regulation of CXCL13 and CCL19 mRNA levels in lung fibroblasts is LTβR-mediated. Furthermore, CSE itself is sufficient to induce CXCL13 expression in cultured lung fibroblasts via LTβR.

In accordance with previous reports (9), the lungs of air-exposed LTα$^{-/-}$ mice were strongly infiltrated with B- and T-cells. Moreover, we found high steady state numbers of CD4^{+} and CD8^{+} T-cells in BALF of air-exposed LTα$^{-/-}$ mice compared to WT mice, in line with earlier research (22). Extensive serology proved all animals to be free of a wide range of viruses and bacteria. Most likely, the lack of lymph nodes in LTα$^{-/-}$ mice causes an accumulation of lymphocytes in organs such as the lungs and the liver, as described before (9).

Lymphoid chemokines are critical for neogenesis and organisation of lymphoid tissue (23;24). The lymphoid chemokines CXCL13 and CCL21 are greatly downregulated in the spleen, but not in the lungs of LTα$^{-/-}$ mice (13;25;26), possibly causing a reversed chemokine gradient and consequent homing of lymphocytes to the lung. We found baseline mRNA levels of CXCL13, CCL19 and CCL20 to be elevated in lungs of air-exposed LTα$^{-/-}$ mice compared to WT mice, which further explains increased recruitment of B- and T-cells to the lungs.

In WT mice, CS exposure increases the expression of CXCL13 and CCL19, a B-cell and T-cell attractant respectively. Furthermore, the presence of CXCL13 in pulmonary lymphoid aggregates of smoke-exposed WT mice indicates a role for this chemokine in ongoing organisation. Whereas LTα is not required for the baseline expression of CXCL13 and

CCL19, it is essential for the CS-induced up-regulation of these lymphoid chemokines. In secondary lymphoid tissue organogenesis, a positive feedback loop mechanism has been described: CXCL13 induces $LT\alpha_1\beta_2$ expression on attracted B-cells through CXCR5 and subsequent stimulation of LTβR on stromal cells, which in turn up-regulates CXCL13 production (27;28). Indeed, we found cultured lung fibroblasts to be responsive to LTβR stimulation through enhanced CXCL13 and CCL19 expression. More importantly, CSE induced *in vitro* CXCL13 expression in WT, but not in $LT\beta R^{-/-}$ lung fibroblasts. In line with a previous report on LTβ expression in stromal cells (29), we detected in these fibroblasts a discreet expression of LTβ, which was up-regulated by CSE, only in WT fibroblasts (data not shown). CSE may thus contain or induce LTβR ligands, implicating the LTβR pathway in CS-induced CXCL13 expression in the lung. However, we can not exclude a general non-responsiveness of $LT\beta R^{-/-}$ lung fibroblasts towards the different stimuli. In figure 8 we propose a mechanism for lymphoid chemokine expression in the lung upon CS exposure.

Interestingly, CXCR5 and CCR7, the receptors for CXCL13 and CCL19 respectively, appear to be important for lymphoid neogenesis in chronic inflammatory autoimmune disease (30). In contrast, the inability of $LT\alpha^{-/-}$ mice to generate a CXCL13- and CCL19-response does not prevent the development of pulmonary lymphoid aggregates upon chronic CS exposure, suggesting other chemokines are involved. We demonstrated that CCL20, a chemokine that attracts immature DCs and lymphocytes, was higher in lungs of air-exposed $LT\alpha^{-/-}$ mice compared to WT mice, and increased further upon chronic CS exposure. CCL20 is thus possibly involved in both steady-state and CS-induced lymphocyte recruitment and lymphoid aggregate formation in $LT\alpha^{-/-}$ mice.

In WT mice, chronic CS exposure induces lymphoid neogenesis with germinal centre formation (5); the latter is known to be LTα-dependent (31). Accordingly, baseline and CS-induced IgA levels in BALF and serum were significantly attenuated in $LT\alpha^{-/-}$ mice compared

to WT animals, whereas LTα$^{-/-}$ mice also showed higher baseline IgM titers in BALF and serum, consistent with a putative Ig isotype switching deficiency. WT mice generated a strong IgA response in BALF upon chronic CS exposure. Similarly, IgA appears to be increased in bronchial secretions of chronic bronchitis patients (32;33). However, when IgA levels are corrected for albumin – to exclude diffusion effects – there is in fact a decrease of indices of local active transport of IgA across the epithelium (32;33), which could relate to reduced expression of epithelial polymeric immunoglobulin receptor/transmembrane secretory component in COPD airways (34). In CS-exposed WT mice, IgA transport towards the airway lumen appeared intact, whereas the strongly reduced S-IgA concentrations in BALF of LTα$^{-/-}$ animals could relate to decreased local IgA synthesis (general defect in class switching to IgA, which could also underlie reduced serum IgA levels) and/or to decreased trans-epithelial transport. Altogether, our B-cell data could indicate impairment in class switch recombination mechanisms in LTα$^{-/-}$ mice, as previously suggested by others (35).

Currently, there is considerable controversy on the role of iNKT cells in airway disease (36;37), a cell population that is profoundly diminished in the periphery of LTα deficient mice (15). Therefore, iNKT cell frequencies were monitored during the course of CS exposure. iNKT cell percentages were significantly reduced in lungs of LTα$^{-/-}$ mice in the chronic experiment. Moreover, subacute CS-exposure increased pulmonary iNKT cell numbers in a LTα-dependent fashion. This is in line with the modulating role of iNKT cells between innate and adaptive immunity, since at this time point (4 weeks), immune responses shift from innate to adaptive in this experimental model of COPD (16). When the adaptive immune system has kicked in, iNKT cell numbers are no longer different between air and CS exposed lungs of WT mice. Corresponding with data from COPD patients (37), our findings do not indicate a role for iNKT cells in the chronic disease model.

In COPD patients, lymphoid aggregates have been correlated with disease severity (6;7). Hypothesizing that the pathogenesis of COPD has an autoimmune component, pulmonary lymphoid aggregates could add to the perpetuating nature of COPD and enhance production of auto-antibodies in the germinal centres. On the other hand, ectopic lymphoid tissue could very well have a local protective role against infections (7). Although LTα polymorphisms are not directly associated with COPD (38;39), potential indirect effects on inflammatory mediators should not be excluded.

In conclusion, we have demonstrated that CS-induced pulmonary lymphoid neogenesis does not require LTα. CS induces the pulmonary expression of lymphoid chemokines CXCL13 and CCL19 in a LTαβ-LTβR-dependent fashion. This murine model of COPD will be useful to further characterize the developing mechanisms and function of CS-induced lymphoid neogenesis.

VI. Acknowledgments

The authors thank Prof. Carl Ware (La Jolla Institute for Allergy and Immunology) for the gift of the LTβR Ab. We thank Dr. Peggy Jacques (Department of Rheumatology, Ghent University Hospital) and Dr. Ann-Sophie Franki (Laboratory for Pharmaceutical Biotechnology, Ghent University) for providing us with advice and reagents. We also thank Greet Barbier, Eliane Castrique, Indra De Borle, Philippe De Gryze, Katleen De Saedeleer, Anouck Goethals, Nicolas Hertsens, Marie-Rose Mouton, Ann Neessen, Christelle Snauwaert and Evelyn Spruyt for their excellent technical assistance.

References

1. Pauwels RA, Buist AS, Calverley PM, Jenkins CR, Hurd SS. Global strategy for the diagnosis, management, and prevention of chronic obstructive pulmonary disease. NHLBI/WHO Global Initiative for Chronic Obstructive Lung Disease (GOLD) Workshop summary. *Am J Respir Crit Care Med* 2001; 163: 1256-1276.

2. Murray CJ, Lopez AD. Alternative projections of mortality and disability by cause 1990-2020: Global Burden of Disease Study. *Lancet* 1997; 349: 1498-1504.

3. Hautamaki RD, Kobayashi DK, Senior RM, Shapiro SD. Requirement for macrophage elastase for cigarette smoke-induced emphysema in mice. *Science* 1997; 277: 2002-2004.

4. Bracke KR, D'hulst AI, Maes T, Moerloose KB, Demedts IK, Lebecque S, Joos GF, Brusselle GG. Cigarette smoke-induced pulmonary inflammation and emphysema are attenuated in CCR6-deficient mice. *J Immunol* 2006; 177: 4350-4359.

5. van der Strate BW, Postma DS, Brandsma CA, Melgert BN, Luinge MA, Geerlings M, Hylkema MN, van den Berg A, Timens W, Kerstjens HA. Cigarette smoke-induced emphysema: A role for the B cell? *Am J Respir Crit Care Med* 2006; 173: 751-758.

6. Hogg JC, Chu F, Utokaparch S, Woods R, Elliott WM, Buzatu L, Cherniack RM, Rogers RM, Sciurba FC, Coxson HO, Pare PD. The nature of small-airway obstruction in chronic obstructive pulmonary disease. *N Engl J Med* 2004; 350: 2645-2653.

7. Hogg JC, Chu FS, Tan WC, Sin DD, Patel SA, Pare PD, Martinez FJ, Rogers RM, Make BJ, Criner GJ, Cherniack RM, Sharafkhaneh A, Luketich JD, Coxson HO, Elliott WM, Sciurba FC. Survival after lung volume reduction in chronic obstructive pulmonary disease: insights from small airway pathology. *Am J Respir Crit Care Med* 2007; 176: 454-459.

8. De Togni P, Goellner J, Ruddle NH, Streeter PR, Fick A, Mariathasan S, Smith SC, Carlson R, Shornick LP, Strauss-Schoenberger J, . Abnormal development of peripheral lymphoid organs in mice deficient in lymphotoxin. *Science* 1994; 264: 703-707.

9. Banks TA, Rouse BT, Kerley MK, Blair PJ, Godfrey VL, Kuklin NA, Bouley DM, Thomas J, Kanangat S, Mucenski ML. Lymphotoxin-alpha-deficient mice. Effects on secondary lymphoid organ development and humoral immune responsiveness. *J Immunol* 1995; 155: 1685-1693.

10. Kratz A, Campos-Neto A, Hanson MS, Ruddle NH. Chronic inflammation caused by lymphotoxin is lymphoid neogenesis. *J Exp Med* 1996; 183: 1461-1472.

11. Sacca R, Cuff CA, Lesslauer W, Ruddle NH. Differential activities of secreted lymphotoxin-alpha3 and membrane lymphotoxin-alpha1beta2 in lymphotoxin-induced inflammation: critical role of TNF receptor 1 signaling. *J Immunol* 1998; 160: 485-491.

12. Crowe PD, VanArsdale TL, Walter BN, Ware CF, Hession C, Ehrenfels B, Browning JL, Din WS, Goodwin RG, Smith CA. A lymphotoxin-beta-specific receptor. *Science* 1994; 264: 707-710.

13. Ngo VN, Korner H, Gunn MD, Schmidt KN, Riminton DS, Cooper MD, Browning JL, Sedgwick JD, Cyster JG. Lymphotoxin alpha/beta and tumor necrosis factor are required for stromal cell expression of homing chemokines in B and T cell areas of the spleen. *J Exp Med* 1999; 189: 403-412.

14. Dejardin E, Droin NM, Delhase M, Haas E, Cao Y, Makris C, Li ZW, Karin M, Ware CF, Green DR. The lymphotoxin-beta receptor induces different patterns of gene expression via two NF-kappaB pathways. *Immunity* 2002; 17: 525-535.

15. Franki AS, Van BK, Dewint P, Hammond KJ, Lambrecht S, Leclercq G, Kronenberg M, Deforce D, Elewaut D. A unique lymphotoxin {alpha}beta-dependent pathway regulates thymic emigration of V{alpha}14 invariant natural killer T cells. *Proc Natl Acad Sci U S A* 2006; 103: 9160-9165.

16. D'hulst AI, Vermaelen KY, Brusselle GG, Joos GF, Pauwels RA. Time course of cigarette smoke-induced pulmonary inflammation in mice. *Eur Respir J* 2005; 26: 204-213.

17. Macdonald G, Kondor N, Yousefi V, Green A, Wong F, Aquino-Parsons C. Reduction of carboxyhaemoglobin levels in the venous blood of cigarette smokers following the administration of carbogen. *Radiother Oncol* 2004; 73: 367-371.

18. Vermaelen K, Pauwels R. Accurate and simple discrimination of mouse pulmonary dendritic cell and macrophage populations by flow cytometry: methodology and new insights. *Cytometry A* 2004; 61: 170-177.

19. Matsuda JL, Naidenko OV, Gapin L, Nakayama T, Taniguchi M, Wang CR, Koezuka Y, Kronenberg M. Tracking the response of natural killer T cells to a glycolipid antigen using CD1d tetramers. *J Exp Med* 2000; 192: 741-754.

20. Futterer A, Mink K, Luz A, Kosco-Vilbois MH, Pfeffer K. The lymphotoxin beta receptor controls organogenesis and affinity maturation in peripheral lymphoid tissues. *Immunity* 1998; 9: 59-70.

21. Bracke K, Cataldo D, Maes T, Gueders M, Noel A, Foidart JM, Brusselle G, Pauwels RA. Matrix metalloproteinase-12 and cathepsin D expression in pulmonary macrophages and dendritic cells of cigarette smoke-exposed mice. *Int Arch Allergy Immunol* 2005; 138: 169-179.

22. Kang HS, Blink SE, Chin RK, Lee Y, Kim O, Weinstock J, Waldschmidt T, Conrad D, Chen B, Solway J, Sperling AI, Fu YX. Lymphotoxin is required for maintaining physiological levels of serum IgE that minimizes Th1-mediated airway inflammation. *J Exp Med* 2003; 198: 1643-1652.

23. Luther SA, Lopez T, Bai W, Hanahan D, Cyster JG. BLC expression in pancreatic islets causes B cell recruitment and lymphotoxin-dependent lymphoid neogenesis. *Immunity* 2000; 12: 471-481.

24. Luther SA, Bidgol A, Hargreaves DC, Schmidt A, Xu Y, Paniyadi J, Matloubian M, Cyster JG. Differing activities of homeostatic chemokines CCL19, CCL21, and CXCL12 in lymphocyte and dendritic cell recruitment and lymphoid neogenesis. *J Immunol* 2002; 169: 424-433.

25. Lo JC, Chin RK, Lee Y, Kang HS, Wang Y, Weinstock JV, Banks T, Ware CF, Franzoso G, Fu YX. Differential regulation of CCL21 in lymphoid/nonlymphoid tissues for effectively attracting T cells to peripheral tissues. *J Clin Invest* 2003; 112: 1495-1505.

26. Moyron-Quiroz JE, Rangel-Moreno J, Kusser K, Hartson L, Sprague F, Goodrich S, Woodland DL, Lund FE, Randall TD. Role of inducible bronchus associated lymphoid tissue (iBALT) in respiratory immunity. *Nat Med* 2004; 10: 927-934.

27. Ansel KM, Ngo VN, Hyman PL, Luther SA, Forster R, Sedgwick JD, Browning JL, Lipp M, Cyster JG. A chemokine-driven positive feedback loop organizes lymphoid follicles. *Nature* 2000; 406: 309-314.

28. Mebius RE. Organogenesis of lymphoid tissues. *Nat Rev Immunol* 2003; 3: 292-303.

29. Cui CY, Hashimoto T, Grivennikov SI, Piao Y, Nedospasov SA, Schlessinger D. Ectodysplasin regulates the lymphotoxin-beta pathway for hair differentiation. *Proc Natl Acad Sci U S A* 2006; 103: 9142-9147.

30. Wengner AM, Hopken UE, Petrow PK, Hartmann S, Schurigt U, Brauer R, Lipp M. CXCR5- and CCR7-dependent lymphoid neogenesis in a murine model of chronic antigen-induced arthritis. *Arthritis Rheum* 2007; 56: 3271-3283.

31. Matsumoto M, Mariathasan S, Nahm MH, Baranyay F, Peschon JJ, Chaplin DD. Role of lymphotoxin and the type I TNF receptor in the formation of germinal centers. *Science* 1996; 271: 1289-1291.

32. Stockley RA, Burnett D. Local IgA production in patients with chronic bronchitis: effect of acute respiratory infection. *Thorax* 1980; 35: 202-206.

33. Atis S, Tutluoglu B, Salepci B, Ocal Z. Serum IgA and secretory IgA levels in bronchial lavages from patients with a variety of respiratory diseases. *J Investig Allergol Clin Immunol* 2001; 11: 112-117.

34. Pilette C, Godding V, Kiss R, Delos M, Verbeken E, Decaestecker C, De PK, Vaerman JP, Decramer M, Sibille Y. Reduced epithelial expression of secretory component in small airways correlates with airflow obstruction in chronic obstructive pulmonary disease. *Am J Respir Crit Care Med* 2001; 163: 185-194.

35. Eugster HP, Muller M, Karrer U, Car BD, Schnyder B, Eng VM, Woerly G, Le HM, di PF, Aguet M, Zinkernagel R, Bluethmann H, Ryffel B. Multiple immune abnormalities in tumor necrosis factor and lymphotoxin-alpha double-deficient mice. *Int Immunol* 1996; 8: 23-36.

36. Akbari O, Faul JL, Hoyte EG, Berry GJ, Wahlstrom J, Kronenberg M, DeKruyff RH, Umetsu DT. CD4+ invariant T-cell-receptor+ natural killer T cells in bronchial asthma. *N Engl J Med* 2006; 354: 1117-1129.

37. Vijayanand P, Seumois G, Pickard C, Powell RM, Angco G, Sammut D, Gadola SD, Friedmann PS, Djukanovic R. Invariant natural killer T cells in asthma and chronic obstructive pulmonary disease. *N Engl J Med* 2007; 356: 1410-1422.

38. Ruse CE, Hill MC, Tobin M, Neale N, Connolly MJ, Parker SG, Wardlaw AJ. Tumour necrosis factor gene complex polymorphisms in chronic obstructive pulmonary disease. *Respir Med* 2007; 101: 340-344.

39. Tanaka G, Sandford AJ, Burkett K, Connett JE, Anthonisen NR, Pare PD, He JQ. Tumour necrosis factor and lymphotoxin A polymorphisms and lung function in smokers. *Eur Respir J* 2007; 29: 34-41.

Figure Legends

FIGURE 1. Total BAL cells and cell differentiation in BAL fluid of wild-type (WT) and LT$\alpha^{-/-}$ mice after subacute (4 weeks) or chronic (24 weeks) exposure to air or cigarette smoke: *A*, total BAL cells; *B*, macrophages; *C*, dendritic cells; *D*, neutrophils; *E*, $CD4^+$ T-cells and *F*, $CD8^+$ T-cells (*A* and *D* were calculated on cytospins; *B*, *C*, *E* and *F* were enumerated by flow cytometry). Results are expressed as mean ± SEM. $n = 8$ animals/group; *, $p < 0.05$; **, $p < 0.01$; ***, $p < 0.001$.

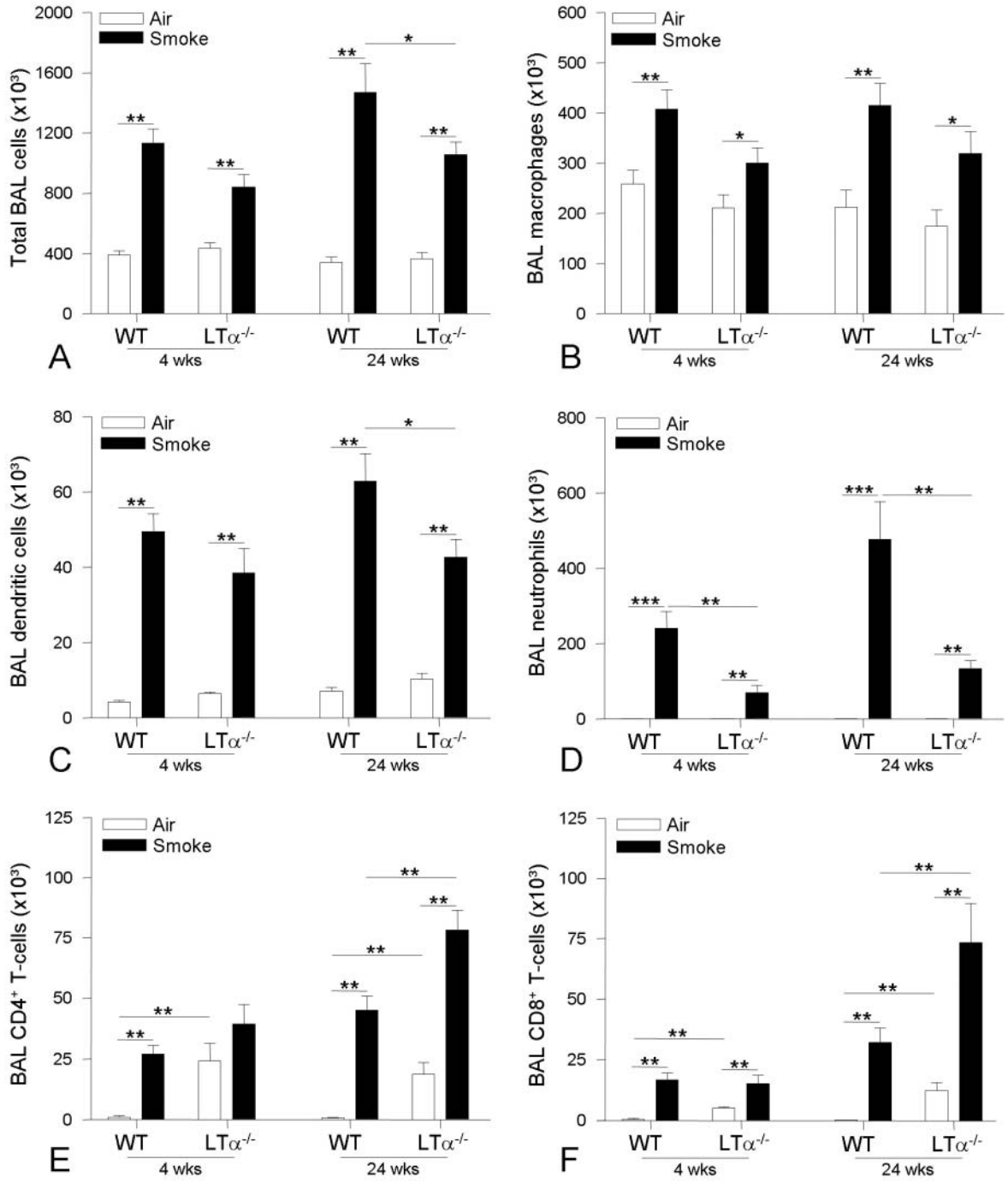

Figure 1.

FIGURE 2. Cell differentiation in the lungs of wild-type (WT) and LTα$^{-/-}$ mice after chronic (24 weeks) exposure to air or cigarette smoke: *A*, macrophages; *B*, dendritic cells; *C*, B-cells; *D*, T-cells; *E*, activated CD4^{+} T-cells and *F*, activated CD8^{+} T-cells (all cell types were

enumerated by flow cytometry). Results are expressed as mean ± SEM. n = 8 animals/group; *, $p < 0.05$; **, $p < 0.01$.

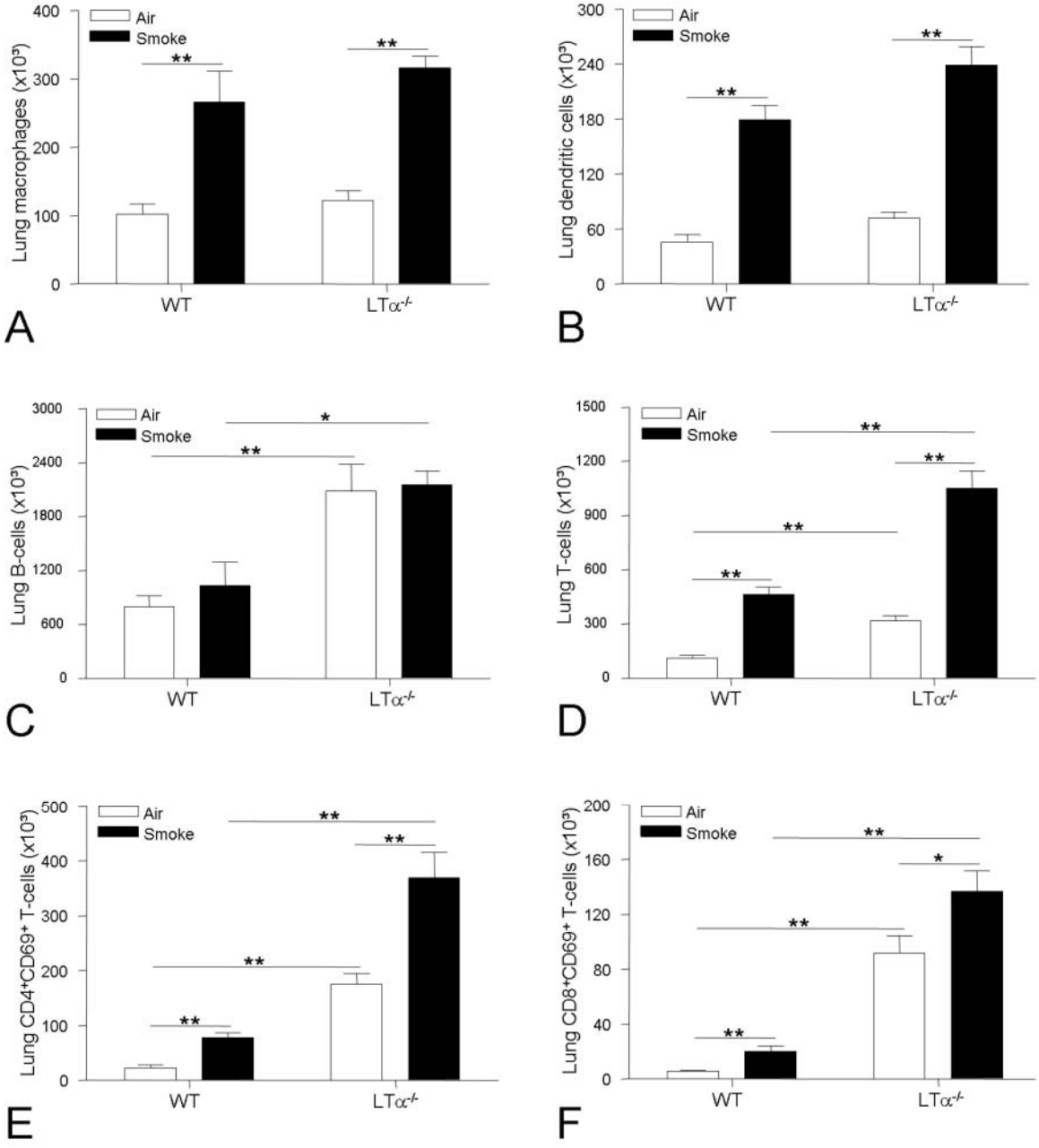

Figure 2.

FIGURE 3. Invariant Natural Killer T (iNKT) cells in lung digests of wild-type (WT) and LTα$^{-/-}$ mice after subacute (4 weeks) or chronic (24 weeks) exposure to air or cigarette smoke, enumerated by flow cytometry. *A*, iNKT cells were stained with APC-conjugated anti-CD3

antibody and PE-conjugated CD1d-tetramer loaded with α-galactosylceramide (α-GalCer). Results are expressed as percentage of total cells (*B* and *D)* and as absolute cell number (*C* and *E*), mean ± SEM. $n = 8$ animals/group; *, $p < 0.05$.

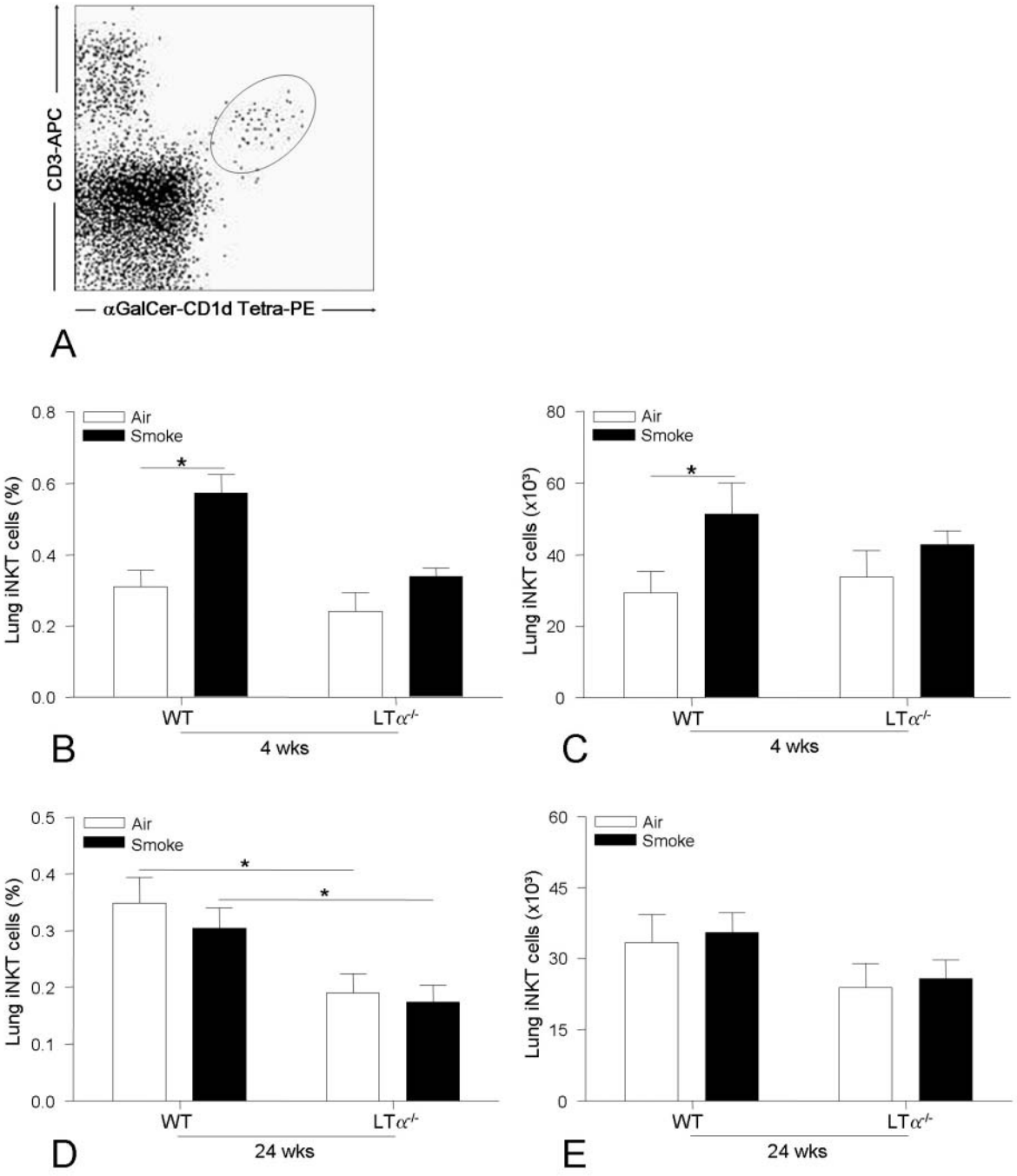

Figure 3.

FIGURE 4. Lymphoid aggregates in lung tissue of wild-type (WT) and LTα$^{-/-}$ mice after chronic (24 weeks) exposure to air or cigarette smoke (CS). *A*, Quantification of peribronchial and perivascular lymphoid aggregates. Results are expressed as mean ± SEM. n = 8 animals/group; **, $p < 0.01$; ***, $p < 0.001$. *B-E*, Photomicrographs of lymphoid aggregates in CD3/B220 immuno-stained lung tissue of air- and smoke-exposed WT and LTα$^{-/-}$ mice at 24 weeks (magnification, x100; brown = CD3 positive cells; blue = B220 positive cells). *B*, air-exposed WT mice; *C*, CS-exposed WT mice; *D*, air-exposed LTα$^{-/-}$ mice; and *E*, CS-exposed LTα$^{-/-}$ mice. Scale bars = 100 μm.

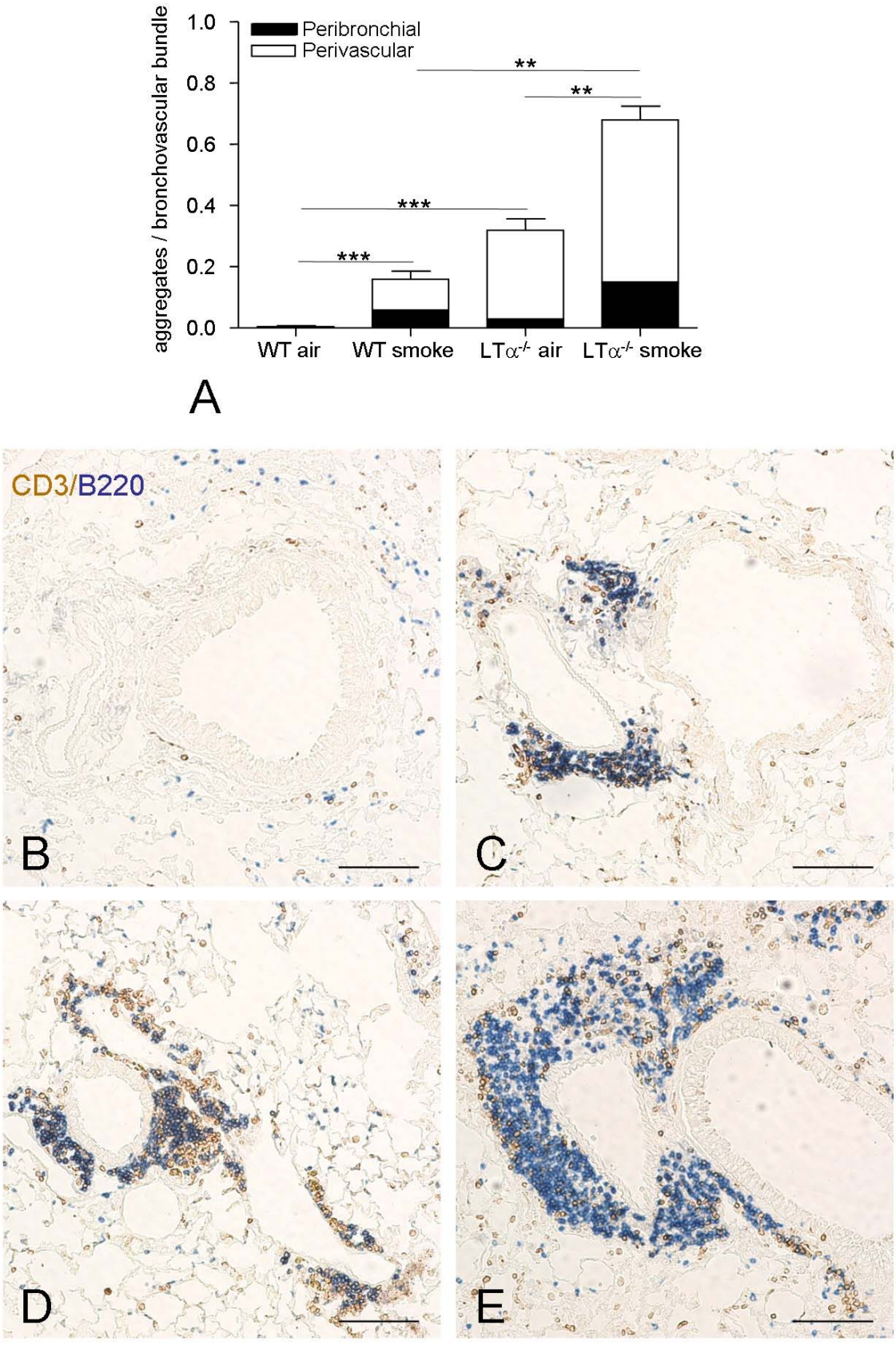
aggregates / bronchovascular bundle
1.0
0.8
0.6
0.4
0.2
0.0
Peribronchial
Perivascular
**
**
***
***
WT air
WT smoke
LTα-/- air
LTα-/- smoke
A
CD3/B220
B
C
D
E

Figure 4.

FIGURE 5. Immunoglobulin A (IgA) levels in serum (*A*), total IgA (*B*) and secretory IgA (*C*) in BAL fluid of wild-type (WT) and LT$\alpha^{-/-}$ mice after chronic (24 weeks) exposure to air or cigarette smoke, as measured by ELISA. IgA titers are expressed as μg/ml and secreted-IgA (S-IgA) levels as corrected optical density (OD) (mean ± SEM). n = 8 animals/group; *, $p < 0.05$; **, $p < 0.01$; ***, $p < 0.001$. Immunoglobulin M (IgM) levels in serum (*D*) and BAL fluid (*E*) of WT and LT$\alpha^{-/-}$ mice after subacute (4 weeks) exposure to air or cigarette smoke, as measured by ELISA. Results are expressed as μg/ml (serum IgM) and ng/ml (BALF IgM), mean ± SEM. n = 8 animals/group; *, $p < 0.05$; **, $p < 0.01$.

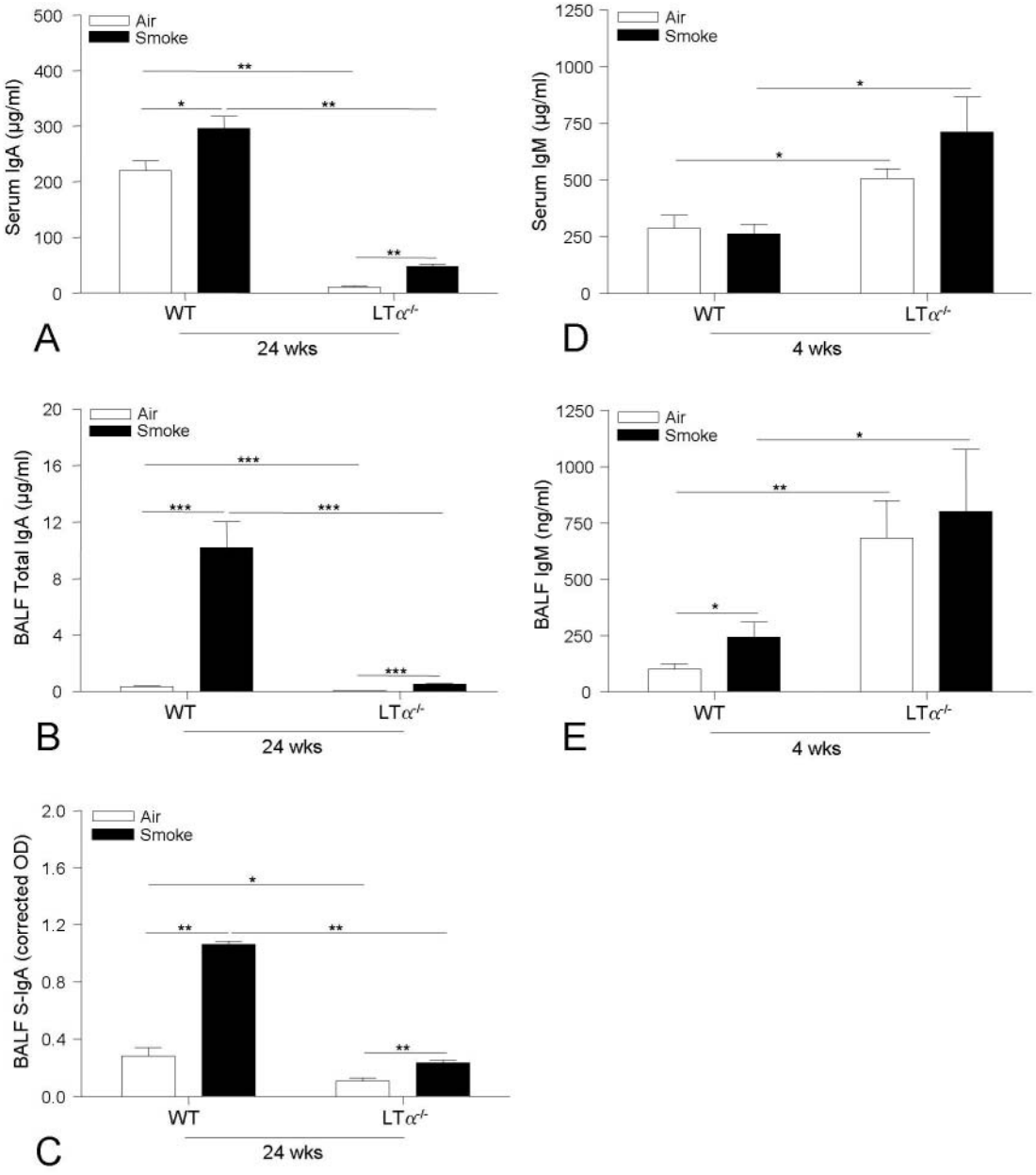

Figure 5.

FIGURE 6. Measurement of chemokines in BAL fluid and lung tissue. mRNA levels of CXCL13 (*A),* CCL19 (*B*) and CCL20 (*C*) in total lung tissue of wild-type (WT) and LTα$^{-/-}$ mice after subacute (4 weeks) or chronic (24 weeks) exposure to air or cigarette smoke, as measured by RT-PCR. Results are expressed as ratio with hprt mRNA (mean ± SEM). $n = 5$ animals/group; *, $p < 0.05$; **, $p < 0.01$. *D*, Protein levels of CXCL13 in BAL fluid of WT and LTα$^{-/-}$ mice after subacute (4 weeks) or chronic (24 weeks) exposure to air or cigarette

smoke, as measured by ELISA. Results are expressed as pg/ml (mean ± SEM). n = 8 animals/group; *, $p < 0.05$; **, $p < 0.01$. *E*, Photomicrographs of a CXCL13-positive lymphoid aggregate in a smoke-exposed WT animal at 24 weeks. Magnification, x100: scale bar = 100 μm; magnification, x400: scale bar = 20 μm.

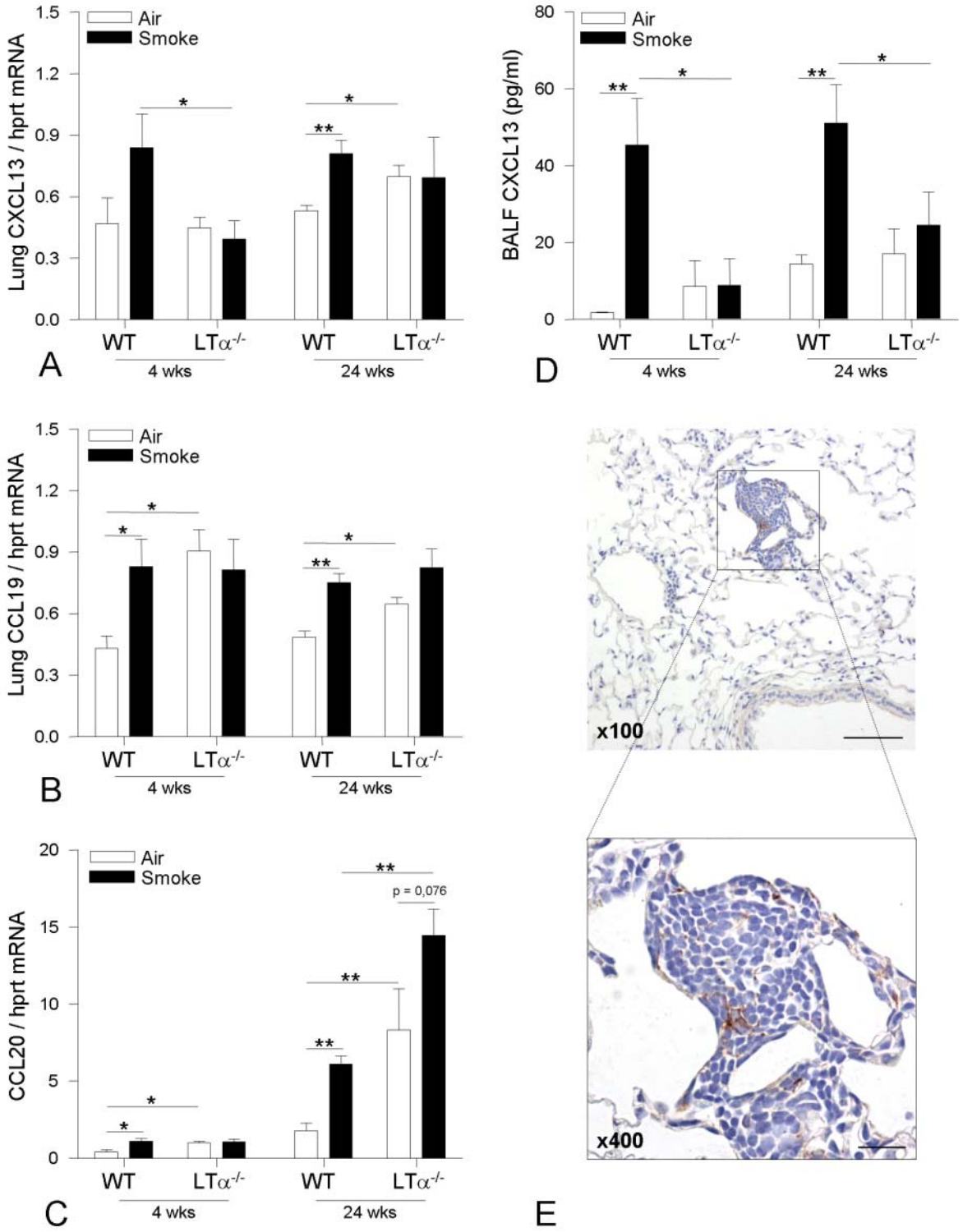

Figure 6.

FIGURE 7. Expression of lymphoid chemokines CXCL13 and CCL19 by lung fibroblasts, in response to LTβR stimulation *in vitro*. *A-D*, Cultured lung fibroblasts were exposed for 48 hours to DMEM, isotype control, agonistic LTβR antibody (Ab), cigarette smoke extract

(CSE) or the combination of LTβR Ab with CSE (Ab+CSE). mRNA levels of CXCL13 (*A* and *B*) and CCL19 (*C* and *D*) in WT and LTβR$^{-/-}$ fibroblasts, as measured by RT-PCR. Results are expressed as ratio with hprt mRNA; mean of 3 experiments ± SEM; *, $p \leq 0.05$.

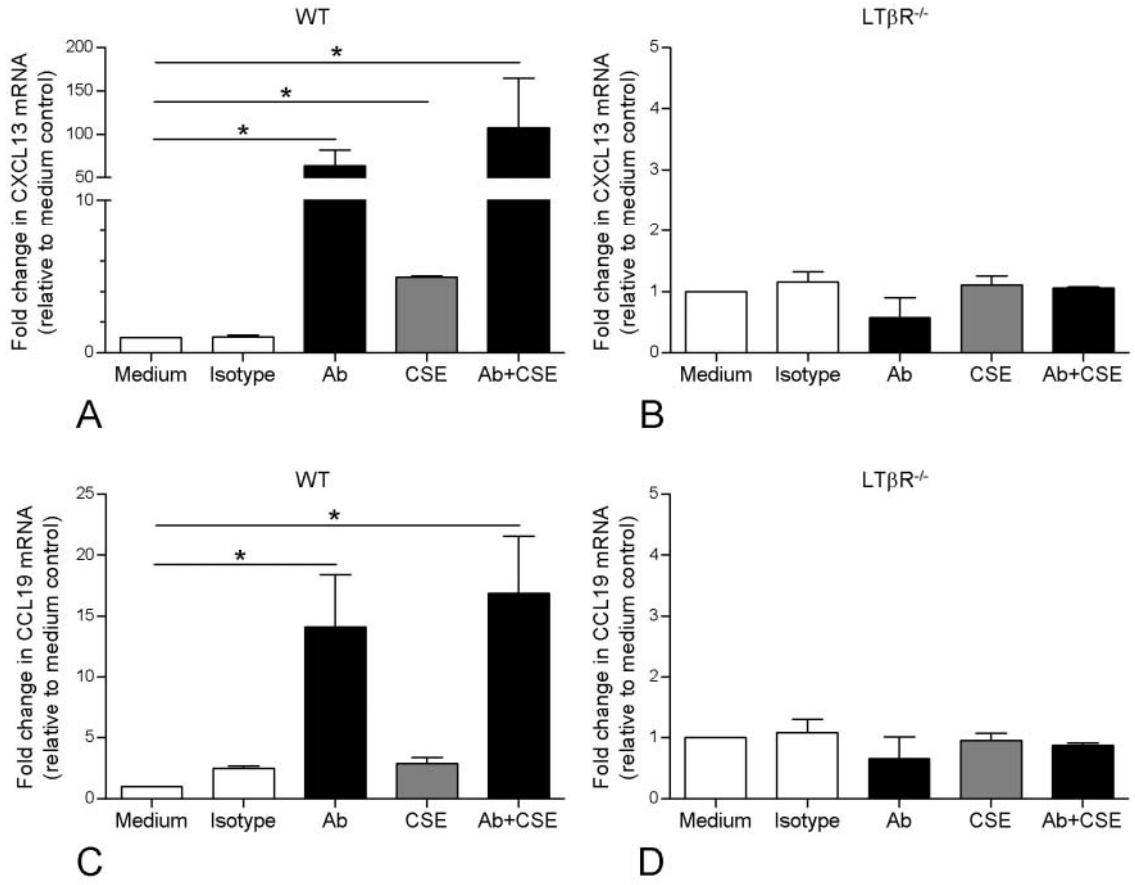

Figure 7.

FIGURE 8. Proposed mechanism for lymphoid chemokine expression in the lung upon CS exposure. CS induces pulmonary inflammation and subsequent expression of LTαβ on lymphocytes, but may also directly stimulate the LTβR on stromal cells, such as lung fibroblasts. LTβR-stimulation leads to the production of CCL19 and CXCL13 which attract DCs and T-cells, and B-cells respectively. Finally, CXCL13 may induce LTαβ on B-cells, creating a positive feedback loop mechanism.

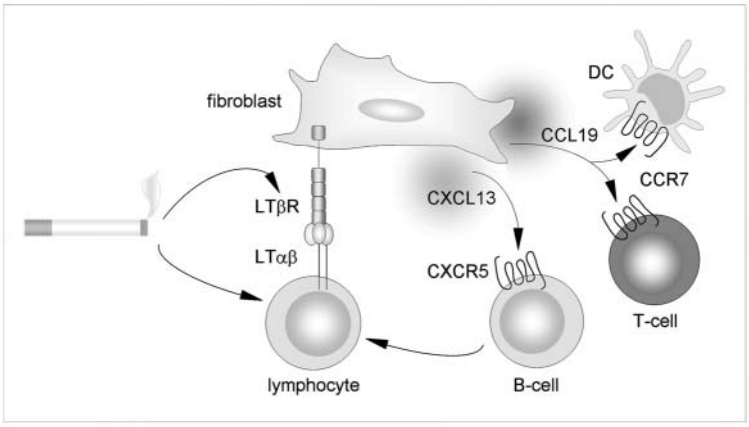
fibroblast
DC
CCL19
CCR7
CXCL13
LTβR
LTαβ
CXCR5
T-cell
lymphocyte
B-cell

Figure 8.